Dimensional analysis of over-reinforced concrete beams in bending

Mauro Corrado, Alberto Carpinteri

Department of Structural and Geotechnical Engineering, Politecnico di Torino, Torino, Italy
E-mail: mauro.corrado@polito.it; alberto.carpinteri@polito.it

Keywords: Dimensional analysis, Reinforced concrete, Nonlinear analysis, Fracture mechanics, Cohesive Crack Model, Concrete crushing.

SUMMARY. In the present paper, Dimensional Analysis is applied to a numerical approach based on Nonlinear Fracture Mechanics in order to obtain a synthetic description of the rotational capacity of reinforced concrete beams in bending, otherwise impossible to be achieved due to the presence of lots of variables and mechanical nonlinearities. Although the proposed model relies on several mechanical properties of concrete and steel and on the beam size, it is demonstrated that only two nondimensional parameters, N_P and N_C, are responsible for the available ductility. Experimental confirmations to the numerical approach are also proposed.

1 INTRODUCTION

A detailed analysis of the mechanical behaviour of reinforced concrete structures during the loading process evidences a series of complex phenomena characterizing the global nonlinearity, namely the concrete fracturing and/or crushing and the steel yielding and/or slippage. For this reason the problem of the rotational capacity of reinforced concrete beams in bending has been faced, both theoretically and experimentally, by several studies each of them focusing on a different aspect. This makes difficult to give a unified and exhaustive description of the physical phenomenon. So far, for instance, the relative neutral axis position at the ultimate condition, x/d, has been chosen as a governing parameter for the rotational capacity. According to this choice, the results of different experimental campaigns have been merged in a ϑ_{PL} versus x/d diagram, as an attempt to obtain a practical design prescription. However, the wide scattering of the results in such a diagram, clearly evidenced in [1], suggests that the nondimensional parameter x/d does not completely describe the considered phenomenon.

In order to overcome such drawbacks, relevant contributions may be given by Dimensional Analysis, based on Buckingham's Π-Theorem [2,3], which permits to clearly connect the mechanical response to dimensionless groups of the variables involved in the phenomenon, rather than to the individual values of them. The most relevant applications in Solids and Fracture Mechanics have concerned the analysis of complete and incomplete physical similarity of strength and toughness in disordered materials [4-9] as well as the study of the incomplete self-similarity in fatigue crack growth [10,11]. According to such studies, different dimensionless numbers have been proposed to govern the stability of progressive cracking:

- the *stress brittleness number* in the case of brittle materials [4]:

$$s = \frac{K_{IC}}{\sigma_u h^{1/2}}, \tag{1}$$

- the *reinforcement brittleness number* in the case of lightly reinforced concrete elements [5]:

$$N_P = \rho_t \frac{\sigma_y h^{1/2}}{K_{IC}}, \tag{2}$$

- and the *energy brittleness number* for quasi-brittle materials [6]:

$$s_E = \frac{\mathcal{G}_F}{\sigma_u h}, \tag{3}$$

where K_{IC} is the material fracture toughness, σ_u is its ultimate tensile strength, $\mathcal{G}_F$ is the fracture energy, ρ_t and σ_y are, respectively, the percentage and the yielding strength of steel reinforcement, and h is a characteristic linear size of the specimen. In all these cases a transition from ductile to softening, or even snap-back, failure is evidenced by decreasing the brittleness number.

In the present paper, Dimensional Analysis is applied to the model proposed by Carpinteri *et al.* [12,13], for the assessment of the rotational capacity of reinforced concrete beams in bending. In particular, it will be demonstrated that only two nondimensional parameters, N_P and N_C, are responsible for the available ductility. Then, experimental confirmations to the numerical approach are also proposed [14].

2 MATHEMATICAL AND NUMERICAL FORMULATION

In this section, the numerical algorithm proposed by Carpinteri *et al.* [12,13] for the analysis of the behaviour of reinforced concrete elements in bending is briefly introduced. This model permits to study a portion of a reinforced concrete beam subjected to a constant bending moment M, as that shown in Fig. 1. This element, having a span to depth ratio equal to unity, is representative of the zone of a beam where a plastic hinge formation takes place. It is assumed that fracturing and crushing processes are fully localized along the mid-span cross-section of the element. This assumption, fully consistent with the crushing phenomenon, also implies that only one equivalent main tensile crack is considered. The loading process is characterized by a crack propagation in tension, a steel yielding and/or slippage and a concrete crushing in compression.

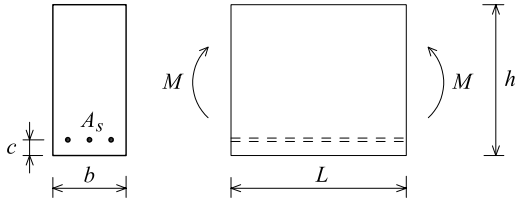

Figure 1: Scheme of a reinforced concrete element.

In the proposed algorithm, the behaviour of concrete in tension is described by means of the well established *Cohesive Crack Model* [15-17], largely used, in the past, to study the ductile-to-brittle transition in plain concrete beams in bending. According to this model, the adopted constitutive law is a stress–strain linear-elastic relationship up to the achievement of the tensile strength, σ_u, for the undamaged zone, and a stress–displacement linear relationship describing the

material in the process zone. The critical crack opening displacement is $w_{cr}^{t} \approx 0.1$ mm, and the fracture energy, $\mathcal{G}_F$, is assumed to vary from 0.050 N/mm to 0.150 N/mm, depending on concrete strength and maximum aggregate diameter, according to the prescriptions in Model Code 90 [18].

As far as modelling of concrete crushing failure is concerned, the *Overlapping Crack Model* introduced by Carpinteri *et al.* [12,13] is adopted. According to such an approach, strongly confirmed by experimental results [19,20], the inelastic deformation in the post-peak regime is described by a fictitious interpenetration of the material, while the remaining part of the specimen undergoes an elastic unloading. As a result, a pair of constitutive laws for concrete in compression is introduced, in close analogy with the *Cohesive Crack Model*: a stress–strain relationship until the compressive strength is achieved (Fig. 2a), and a stress–displacement (overlapping) relationship describing the phenomenon of concrete crushing (Fig. 2b). The latter law describes how the stress in the damaged material decreases from its maximum value to zero as the fictitious interpenetration increases from zero to the critical value, w_{cr}^{c}. It is worth noting that the crushing energy, $\mathcal{G}_C$, which is a surface dissipated energy, defined as the area below the post-peak softening curve in Fig. 2b, can be assumed as a true material property, since it is not affected by the structural size. An empirical equation for calculating the crushing energy has been recently proposed by Suzuki *et al.* [21], taking into account the confined concrete compression strength by means of the stirrups yield strength and the stirrups volumetric content. By varying the concrete compressive strength from 20 to 90 MPa, the crushing energy ranges from 30 to 58 N/mm. The critical value for the crushing interpenetration is experimentally found to be approximately equal to 1 mm (see also [20]). It is worth noting that this value is a decreasing function of the compressive strength, in agreement with the more brittle response exhibited by high strength concrete. On the contrary, we observe that, in the case of concrete confinement, the crushing energy, and the corresponding critical value for crushing interpenetration, considerably increase.

As far as the behaviour of steel reinforcement is concerned, a constitutive relationship between the reinforcement reaction and the crack opening displacement is introduced instead of the classical σ–ε laws, since the kinematics of the mid-span cross-section is described by means of displacements, and not by strains. In the proposed model, stress vs. crack opening displacement relationships have been obtained through a bond-slip analysis between concrete and steel. In particular, the integration of the differential slip over the transfer length, l_{tr}, is equal to half the crack opening at the reinforcement level, whereas the integration of the bond stresses gives the reinforcement reaction. In order to simplify the calculation, the obtained stress-displacement laws are transformed into elastic-perfectly plastic relationships, with a linear branch until the yield stress –corresponding to the critical crack opening for steel, w_y– is achieved, followed by a plateau.

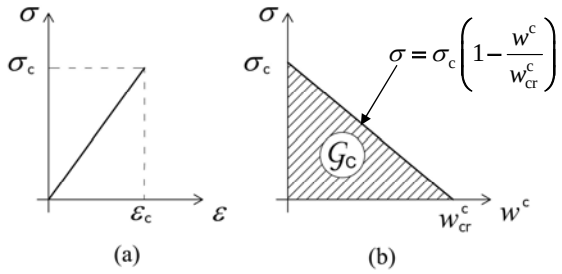

Figure 2: Overlapping Crack Model for concrete in compression: linear-elastic σ–ε law (a); post-peak softening σ–w relationship (b).

2.1 *Numerical algorithm*

A discrete form of the elastic equations governing the mechanical response of the two half-beams is herein introduced. The reinforced concrete member shown in Fig. 1 is considered as constituted by two symmetrical elements characterized by an elastic behavior, and connected by means of *n* pairs of nodes. (Fig. 3a). In this approach, all the mechanical nonlinearities are localized in the mid-span cross-section, where cohesive and overlapping stresses are replaced by equivalent nodal forces, F_i, by integrating the corresponding stresses over the nodal spacing. Such nodal forces depend on the nodal opening or closing displacements according to the cohesive or overlapping softening laws previously introduced.

With reference to Fig. 3a, the horizontal forces, F_i, acting at the i-th node along the mid-span cross-section can be computed as follows:

$$\{F\} = [K_w]\{w\} + \{K_M\}M \tag{4}$$

where $\{F\}$ is the vector of nodal forces, $[K_w]$ is the matrix of the coefficients of influence for the nodal displacements, $\{w\}$ is the vector of nodal displacements, $\{K_M\}$ is the vector of the coefficients of influence for the applied moment M.

In the generic situation shown in Fig. 3b, the following equations can be considered:

$$F_i = 0; \qquad \text{for i} = 1, 2, \ldots, (j-1); \quad i \neq r \tag{5a}$$

$$F_i = F_u\left(1 - \frac{w_i^t}{w_{cr}^t}\right); \qquad \text{for i} = j, \ldots, (m-1); \quad i \neq r \tag{5b}$$

$$w_i = 0; \qquad \text{for i} = m, \ldots, p \tag{5c}$$

$$F_i = F_c\left(1 - \frac{w_i^c}{w_{cr}^c}\right); \qquad \text{for i} = (p+1), \ldots, n \tag{5d}$$

$$F_r = f(w_r); \qquad \text{for i} = r. \tag{5e}$$

where: j represents the real crack tip, m represents the fictitious crack tip, p is the fictitious overlapping tip and r is the node corresponding to the steel reinforcement (see Fig. 3b).

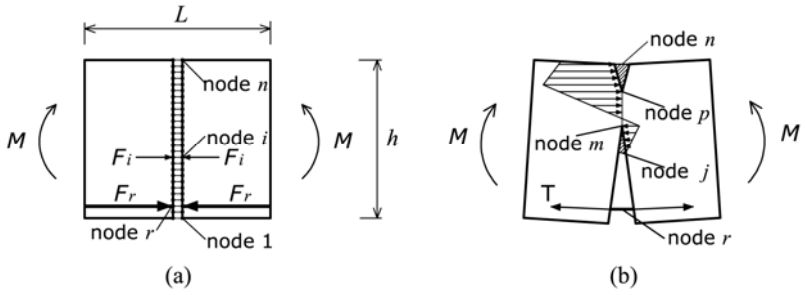

Figure 3: Finite element nodes (a); and force distribution with cohesive crack in tension and crushing in compression (b) along the mid-span cross-section.

Equations (4) and (5) constitute a linear algebraic system of ($2n$) equations in ($2n$+1) unknowns, namely $\{F\}$, $\{w\}$ and M. The necessary additional equation derives from the strength criterion adopted for crack or crushing propagation. At each step of the loading process, in fact, either the force in the fictitious crack tip, m, equals the ultimate tensile force, or the force in the fictitious crushing tip, p, equals the ultimate compressive force. It is important to note that the condition for crack propagation (corresponding to the achievement of the tensile strength at the fictitious crack tip, m) does not imply that the compressive strength is reached at the corresponding overlapping crack tip, p, and viceversa. Hence, the driving parameter of the process is the tip that in the considered step has reached the limit resistance. Only this tip is moved when passing to the next step. This criterion will ensure the uniqueness of the solution on the basis of physical arguments.

Finally, at each step of the algorithm, the localized beam rotation, ϑ, is computed as follows:

$$\vartheta = \{D_w\}^T \{w\} + D_M M \tag{6}$$

where $\{D_w\}$ is the vector of the coefficients of influence for the nodal displacements and D_M is the coefficient of influence for the applied moment.

It is worth noting that Eqs. (4) and (6) permit to analyse the fracturing and crushing processes of the mid-span cross-section taking into account the elastic behaviour of the reinforced concrete member. To this aim, all the coefficients are computed *a priori* using a finite element analysis.

3 APPLICATION OF DIMENSIONAL ANALYSIS TO THE FLEXURAL BEHAVIOUR OF REINFORCED CONCRETE BEAMS

In any practical physical study, we attempt to obtain relationships among the quantities that characterise the phenomenon being studied. Thus, the problem always reduces to determine relationships of the form:

$$q = \Phi\ (q_1, q_2, \ldots, q_n; r_1, r_2, \ldots, r_k) \tag{7}$$

where q is the quantity being determined in the study, q_i and r_i are, respectively, dimensional and nondimensional quantities that are assumed to be given. It is worth noting that, generally, function Φ is not analytically obtainable, although an empirical relationship may be obtained by means of best-fitting procedure, if several results are available varying the parameters of the problem (see [8,9]). On the other hand, we can reduce the number of the governing parameters in order to obtain a synthetic description of the problem. The application of Buckingham's Π-Theorem for physical similitude and scale modelling, in particular, permits to minimize the dimension space of the primary variables, in which the physical phenomenon might be studied, by combining them into dimensionless groups.

When flexural behaviour of reinforced concrete beams is studied, according to the numerical model proposed in the previous section, the functional relationship is the following:

$$M = \Phi\ (\sigma_u, \mathcal{G}_F, \sigma_c, \mathcal{G}_C, E_c, \sigma_y, \rho_t, h; b/h, L/h, \vartheta), \tag{8}$$

where M is the resistant bending moment, σ_u, $\mathcal{G}_F$, σ_c, $\mathcal{G}_C$ and E_c are, respectively, the tensile strength, the fracture energy, the compressive strength, the crushing energy, and the elastic modulus of concrete, σ_y and ρ_t represent the yield strength and the percentage of the tensile

reinforcement, h is the characteristic size of the body, b/h and L/h define the geometry of the sample according to Fig. 1, and ϑ is the local rotation of the element. Since we are interested in the rotational capacity of over-reinforced concrete beams, the set of variables can be reduced as follows:

$$\mathrm{M} = \Phi\,(\sigma_c,\ \mathcal{G}_C,\ E_c,\ \sigma_y,\ \rho_t,\ h;\ \vartheta), \tag{9}$$

where the parameters describing the behaviour of concrete in tension, σ_u and $\mathcal{G}_F$, are not explicitly considered, since they affect only the ascending branch of the moment versus rotation response and they not influence the level and the extension of the plastic plateau. On the other hand, only the beam depth, h, is considered, since the geometrical ratios of the samples , b/h and L/h, are assumed to be constant in the present study.

The application of Buckingham's Π-Theorem to Eq. (9) yields the following relationship:

$$\frac{M}{h^{2.5}\sqrt{\mathcal{G}_C E_c}} = \Phi_1\left(\frac{\sigma_c h^{0.5}}{\sqrt{\mathcal{G}_C E_c}}, \rho_t \frac{\sigma_y h^{0.5}}{\sqrt{\mathcal{G}_C E_c}}, \vartheta \frac{E_c h^{0.5}}{\sqrt{\mathcal{G}_C E_c}}\right) \tag{10}$$

if h and $\sqrt{\mathcal{G}_C E_c}$ are assumed as the dimensionally independent variables. It is worth noting that the former parameter is representative of the size-scale of the specimen, whereas the latter is a material property. In particular, $\sqrt{\mathcal{G}_C E_c}$ can be physically interpreted as the concrete toughness in compression. Its expression, in fact, is analogously to that of the fracture toughness, K_{IC}, defined in terms of the fracture energy and the elastic modulus of the material. As a consequence, the dimensionless functional relationship for the proposed model becomes:

$$\tilde{M} = \Phi_1\left(N_C, N_P, \vartheta_n\right), \tag{11}$$

where:

$$N_P = \rho_t \frac{\sigma_y h^{0.5}}{\sqrt{\mathcal{G}_C E_c}} \tag{12}$$

and

$$N_C = \frac{\sigma_c h^{0.5}}{\sqrt{\mathcal{G}_C E_c}}, \tag{13}$$

are the governing nondimensional numbers, $\tilde{M}$ is the nondimensional bending moment, and ϑ_n is the normalized local rotation. As a result of the Dimensional Analysis, according to Eq. (11), we expect that the structural response, in terms of nondimensional moment versus normalized rotation, is only a function of the dimensionless numbers N_P and N_C.

4 INTERPRETATION OF NUMERICAL AND EXPERIMENTAL RESULTS BASED ON DIMENSIONAL ANALYSIS

In this section, an original interpretation of numerical and experimental results is proposed in order to obtain a unified and exhaustive description of the effects of materials and geometrical properties on the flexural behaviour of reinforced concrete beams. As a confirmation of the analytical results obtained through dimensional analysis, numerical simulations have been carried

out on beams characterised by values of N_P = 0.074 and N_C = 0.630, although different geometrical and mechanical parameters have been assigned, as reported in Fig. 4a. As we can expect, the obtained numerical results, expressed by the nondimensional moment versus normalised rotation diagram shown in Fig. 4b, converge to a single curve, putting into evidence a complete physical similarity in the flexural behaviour by varying the structural dimensions, when N_P and N_C are kept constant. This implies that the analysis of the mechanical behaviour can be profitably carried out on the basis of the two nondimensional numbers, instead of the single geometrical and mechanical parameters. According to this, the numerical simulations for values of N_P ranging from 0.049 up to 0.329, N_C being kept equal to 0.791, are shown in Fig. 5. It is worth noting that, in practical applications, typical values for N_P range from 0.004 up to 0.360, whereas N_C varies from 0.2 up to 3.5. A clear decrement in the rotational capacity is evidenced with a reduction in the plastic plateau as the value of N_P increases. Such a trend can be easily interpreted through an increment in the steel percentage, ρ_t, which appears only in the expression of N_P and not in that of N_C. Note that the ultimate rotation is clearly identified by a softening or even a snap-back branch at the end of the plastic plateau, due to the nonlinear behaviour of concrete in compression.

beam	b	h	σ_y	ρ_t	σ_c	$\mathcal{G}_C$	E_c
	[m]	[m]	[MPa]	[%]	[MPa]	[N/mm]	[GPa]
A	0.05	0.1		2.94	100.0	55.0	46.32
B	0.1	0.2		1.77	60.0	46.9	39.07
C	0.2	0.4	400	1.35	46.0	60.0	35.76
D	0.4	0.8		0.90	30.5	60.0	31.18
E	0.5	1.0		0.58	20.0	37.0	27.09

(a)

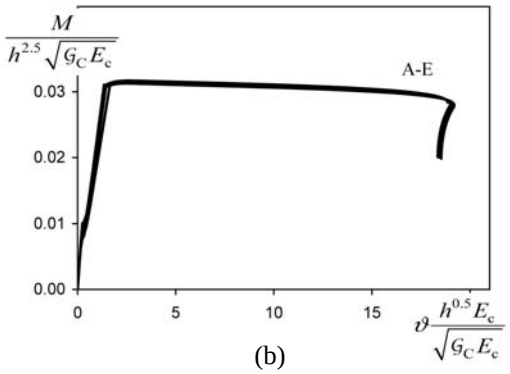

(b)

Figure 4: Mechanical and geometrical parameters (a); and nondimensional moment vs. normalised rotation response (b) of beams characterised by N_P = 0.074 and N_C = 0.630.

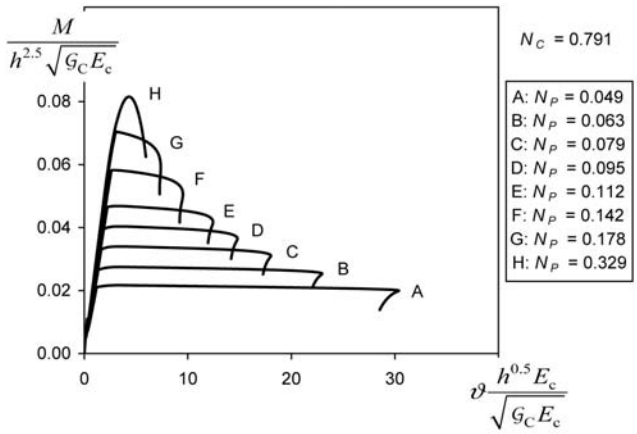

Figure 5: Dimensionless moment vs. normalized rotation diagrams for N_C = 0.791 and different N_P.

On the other hand, the curves in Fig. 6 are related to values of N_C varying from 0.303 up to 2.385 and N_P = 0.109. In this case, the rotational capacity is an increasing function of N_C, as well as of the concrete compressive strength, σ_c. Correspondingly, a more unstable response after the ultimate rotation is also predicted by a more severe snap-back branch.

In order to give an experimental validation to the analytical and numerical approach proposed in the present paper, the bending tests carried out by Bosco and Debernardi [14] on simply supported reinforced concrete beams –loaded by three equal loads arranged symmetrically to the mid-span– are herein considered. The mechanical and geometrical parameters are reported in Tab. 1. The plastic rotations, ϑ_{PL}, of the central beam portion characterised by a length to depth ratio equal to unity, as a function of the relative neutral axis position, x/d, are shown in Fig. 7a. Such results evidence a different trend of the rotational capacity by varying the beam depth from 0.2 m up to 0.6 m. The shallower beams, in fact, exhibit a higher ductility than the deeper ones. These different results collapse onto a single curve in the normalised plastic rotation vs. N_P diagram shown in Fig. 7b. In this case, based on the curves shown in Fig. 6, the nondimensional parameter N_C is not considered, since it exhibits a small variation for the considered beams. The results of the

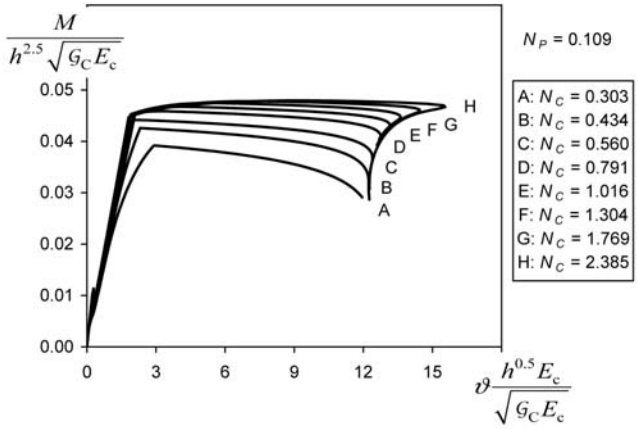

Figure 6. Dimensionless moment vs. normalized rotation diagrams for N_P = 0.109 and different N_C.

beam	b	h	σ_y	ρ_t	σ_c	G_C	E_c	N_P	N_C	x/d	ϑ_{PL}
	[mm]	[mm]	[MPa]	[%]	[MPa]	[N/mm]	[MPa]				[mrad]
T1A3				0.57				0.039		0.226	73.93
T2A3	100	200	600	1.13	30.9	50.0	30000	0.078	0.282	0.335	64.64
T3A3				1.70				0.118		0.600	7.56
T4A3				0.28				0.033		0.115	67.06
T5A3	200	400	600	0.57	30.9	35.0	30000	0.067	0.564	0.229	122.39
T6A3				1.13				0.013		0.462	14.82
T7A3				1.70				0.199		0.636	2.50
T8A3				0.13				0.016		0.108	23.47
T9A3	300	600	600	0.25	30.9	48.0	30000	0.031	0.496	0.147	52.30
T10A3				0.57				0.069		0.237	32.41
T11A3				1.13				0.138		0.488	8.50

Table 1. Mechanical and geometrical parameters of the beams tested by Bosco and Debernardi[14].

numerical simulations carried out with the proposed model are also represented in Fig. 7b by the not filled in symbols. Generally, a good agreement is obtained between numerical and experimental results. For low values of N_P, up to about 0.03, the global collapse is due to steel failure, and $\vartheta_{PL,n}$ is an increasing function of size and steel reinforcement. On the contrary, for higher values of N_P, when the collapse is due to concrete crushing, $\vartheta_{PL,n}$ becomes a decreasing function of size and steel reinforcement.

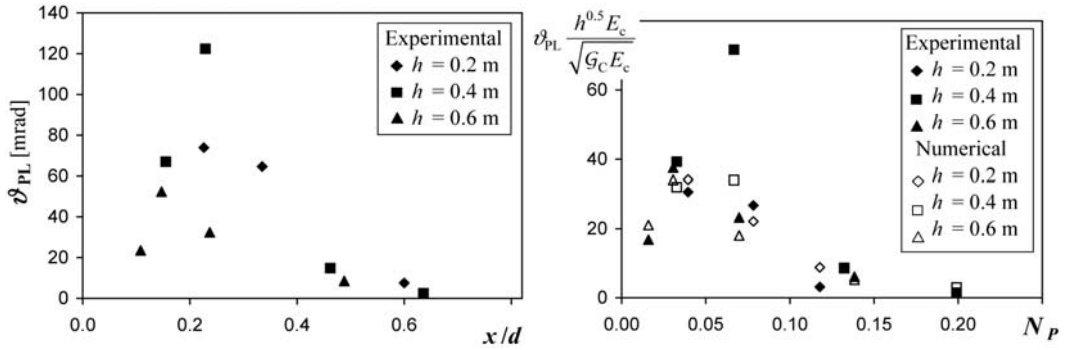

(a) (b)

Figure 7: Experimental [14] plastic rotations vs. x/d diagram (a); experimental [14] and numerical normalised rotations vs. nondimensional number N_P diagram (b).

5 CONCLUSIONS

The application of Dimensional Analysis to the study of the rotational capacity of plastic hinges permits to govern the flexural behaviour of over-reinforced concrete beams by means of two nondimensional numbers, N_P and N_C, combinations of the mechanical and the geometrical parameters. The physical similitude in the nondimensional moment versus normalized rotation diagram evidenced when the two brittleness numbers are kept constant can be profitably used to give new interpretation of experimental results, as proved in Fig. 7a,b. In particular, the diagram in Fig. 7b, permits to describe with a single curve the effect of the structural dimension and the steel reinforcement on the rotational capacity, whereas the analogous ones proposed by Model Code 90 [18], with different variables on the horizontal and vertical axis, completely disregard the size-scale effects. The normalized rotation is a decreasing function of N_P, N_C being kept constant, whereas it increases by increasing the value of N_C, N_P being kept constant.

Finally, Dimensional Analysis is a useful tool in experimental investigations. According to Fig. 4, for instance, we can assert that, in order to predict the structural behaviour of a beam element with depth h = 1 m, bar reinforcement percentage ρ_t = 0.58%, concrete compressive strength σ_c = 20 MPa, crushing energy G_C = 37 N/mm and elastic modulus E_c = 27088 N/mm^2, by an experimental test on a beam scaled 1:10 (h = 0.1 m), the latter should have ρ_t = 2.94%, σ_c = 100 MPa, G_C = 55 N/mm, E_c = 46320 N/mm^2.

References

[1] Siviero, E., "Rotation capacity of monodimensional members in structural concrete," *CEB Bulletin d'Information* **105**, 206-222 (1974).

[2] Buckingham, E., "Model experiments and the form of empirical equations," *ASME Trans.*, **37**, 263-296 (1915).
[3] Barenblatt, G.I., *Scaling, self-similarity, and intermediate asymptotics*, Cambridge University Press, Cambridge, UK, (1996).
[4] Carpinteri, A., "Notch sensitivity in fracture testing of aggregative materials," *Eng. Fract. Mech.*, **16**, 467-481 (1982).
[5] Carpinteri, A., "Stability of fracturing process in RC beams," *J. Struct. Eng.*, **110**, 544-558 (1984).
[6] Carpinteri, A., "Size-scale transition from ductile to brittle failure: structural response vs. crack growth resistance curve," *Int. J. Fract.*, **51**, 175-186 (1991).
[7] Carpinteri, A., Ferro, G. and Ventura, G., "Size effects on flexural response of reinforced concrete elements with a nonlinear matrix," *Eng. Fract. Mech.*, **70**, 995-1013 (2003).
[8] Phatak, D.R. and Deshpande, N.P., "Prediction of 28 days compressive strength of 53-grade cements using dimensional analysis," *J. Mater. Civil Engrg.*, **17**, 733-735 (2005).
[9] Phatak, D.R. and Dhonde, H.B., "Dimensional analysis of reinforced concrete beams subjected to pure torsion," *J. Struct. Eng.*, **129**, 1559-1563 (2003).
[10] Barenblatt, G.I. and Botvina, L.R., "Incomplete self-similarity of fatigue in the linear range of fatigue crack growth," *Fatigue Fract. Engng. Mater. Struct.*, **3**, 193-202 (1980).
[11] Ciavarella, M., Paggi, M. and Carpinteri, A., "One, no one, and one hundred thousand crack propagation laws: a generalized Barenblatt and Botvina dimensional analysis approach to fatigue crack growth," *J. Mech. Physics of Solids*., **56**, 3416-3432 (2008).
[12] Carpinteri, A., Corrado, M., Paggi, M. and Mancini, G., "Cohesive versus overlapping crack model for a size effect analysis of RC elements in bending," in *Proc. 6th International FraMCoS Conference* (vol. 2 London, Taylor & Francis), Catania, Italy 2007, 655-663 (2007).
[13] Carpinteri, A., Corrado, M., Paggi, M. and Mancini. G., "New model for the analysis of size-scale effects on the ductility of reinforced concrete elements in bending," *J. Eng. Mech.*, **135**, 221-229 (2009).
[14] Bosco, C. and Debernardi, P.G., "Influence of some basic parameters on the plastic rotation of reinforced concrete elements," *CEB Bulletin d'Information*, **218**, 25-44 (1993).
[15] Hillerborg, A., Modeer, M. and Petersson, P.E., "Analysis of crack formation and crack growth in concrete by means of fracture mechanics and finite elements," *Cement Concr. Res*., **6**, 773-782 (1976).
[16] Carpinteri, A., "Interpretation of the Griffith instability as a bifurcation of the global equilibrium," in *Proc. of a NATO Advanced Research Workshop* (Dordrecht, Martinus Nijhoff Publishers), Evanston, USA, 1984, 287-316 (1985).
[17] Carpinteri, A., "Size effects on strength, toughness, and ductility," *J. Eng. Mech.*, **115**, 1375-92 (1989).
[18] Comité Euro-International du Béton, *CEB-FIP Model Code 1990*, Thomas Telford Ltd, Lausanne, CEB Bulletin d'Information, **213/214** (1993).
[19] van Vliet, M. and van Mier, J., "Experimental investigation of concrete fracture under uniaxial compression," *Mech. Cohesive-Frictional Mater.*, **1**, 115-127 (1996).
[20] Jansen, D.C. and Shah, S.P., "Effect of length on compressive strain softening of concrete," *J. Eng. Mech.*, **123**, 25-35 (1997).
[21] Suzuki, M., Akiyama, M., Matsuzaki, H. and Dang, T.H., "Concentric loading test of RC columns with normal- and high-strength materials and averaged stress-strain model for confined concrete considering compressive fracture energy," in *Proc. 2nd fib Congress*, Naples, Italy, 2006, Paper ID 3-13 on CD-ROM, 2006.